

Background :

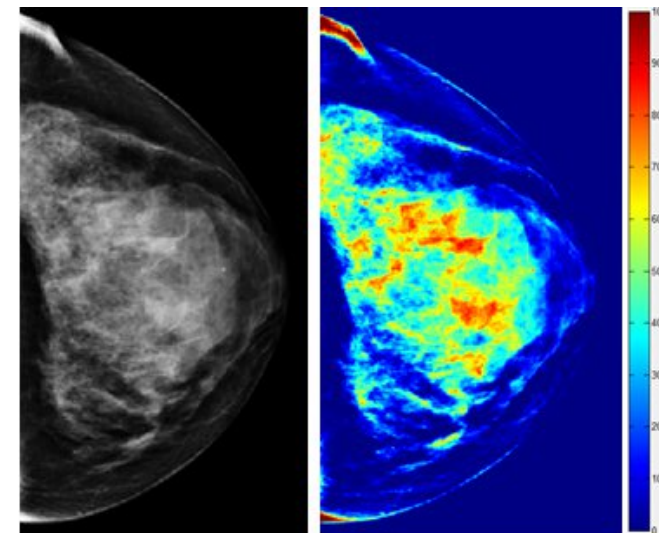
- Breast cancer: Most common cancer in women
- Early detection methods can improve overall survival
- Current risk assessment models do not accurately predict individual risk
- Radiographic image features in mammograms change as suspicious breast abnormalities develop

Targets:

- Develop new image feature analysis-based cancer risk prediction model
- New risk model that takes prior screenings into account
- New model for short-term individualized screening recommendations (e.g., 6 months to 5 years)

Speaker:

- Maxine Tan, PhD, Monash University Malaysia



Example of segmented fibro-glandular tissue volume on a BIRADS D digital mammogram

Project Members :

Maxine Tan, PhD,
Monash
University,
Malaysia



Hwee Kuan Lee,
PhD,
A*STAR,
Singapore



Kartini Rahmat,
MD,
University of
Malaya,
Malaysia

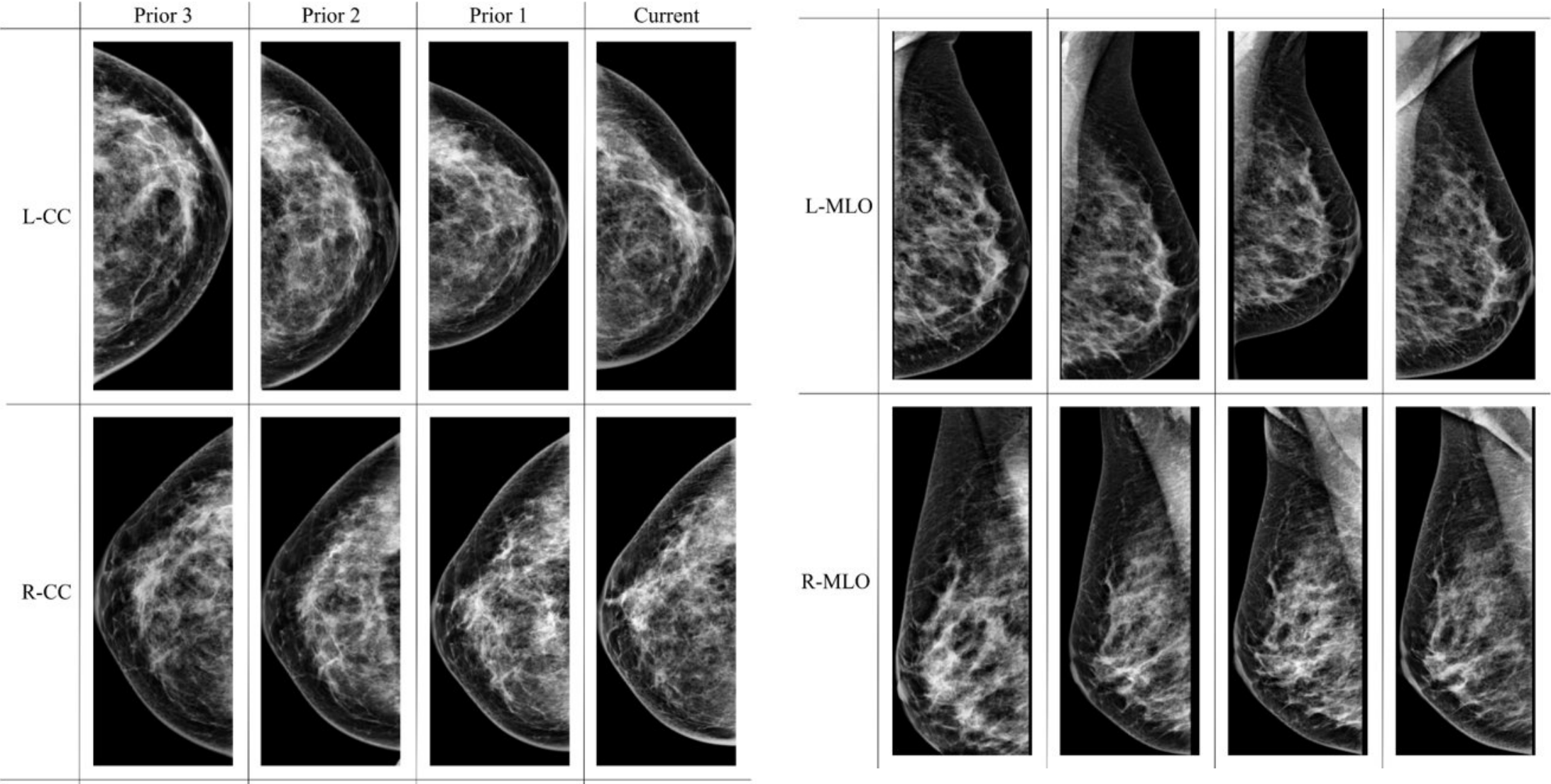


Project Duration :

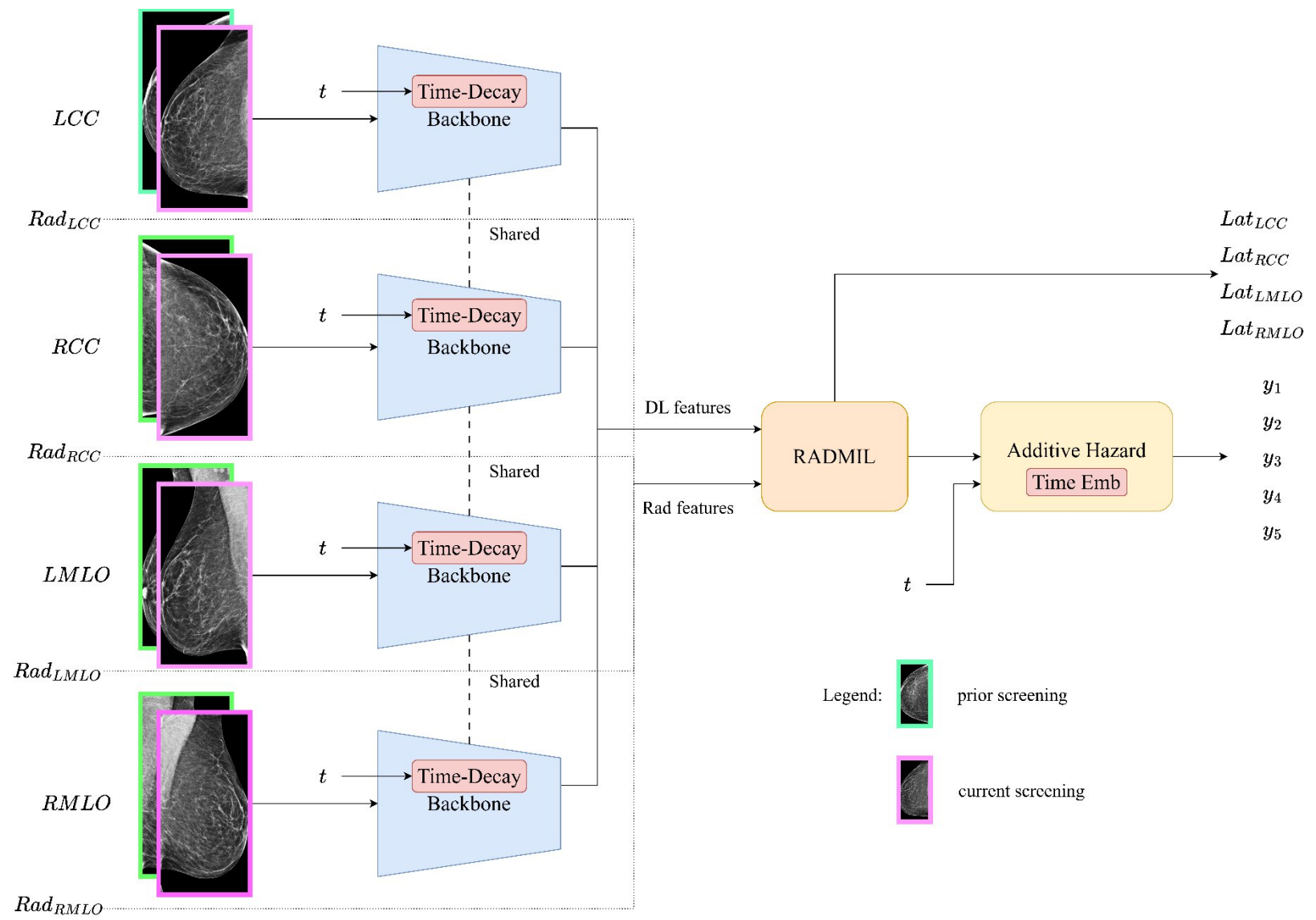
- 23 months

Project Budget:

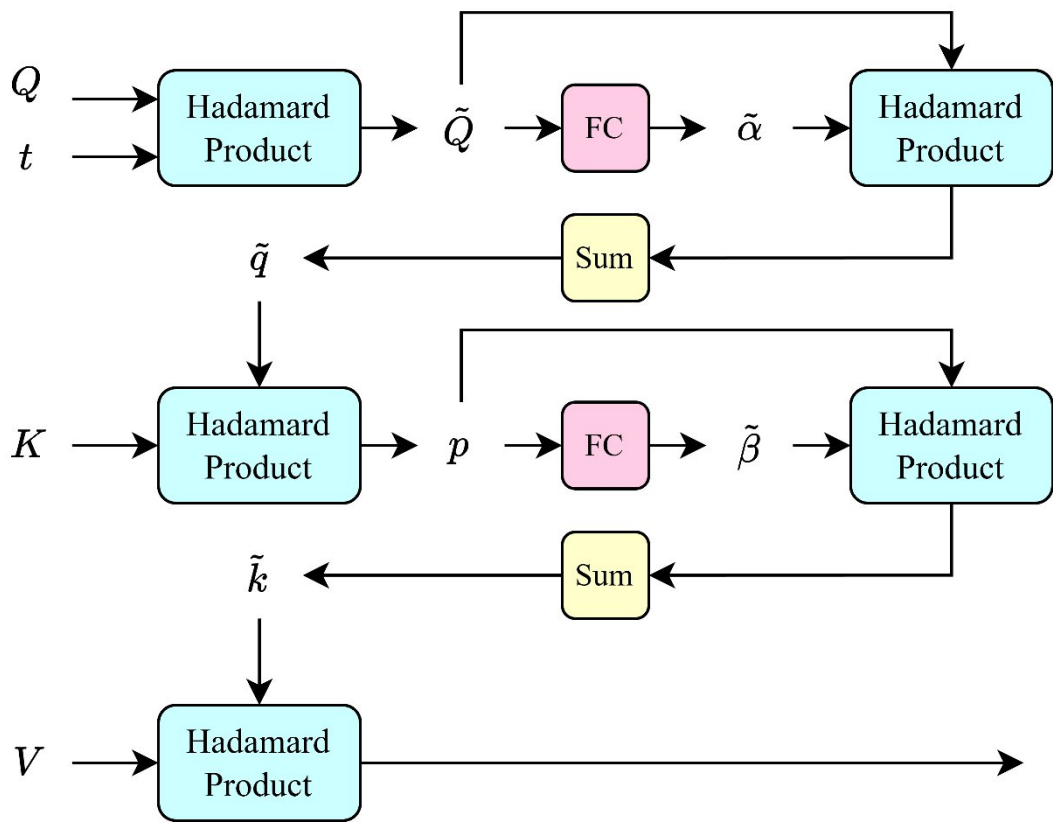
- USD 29,510



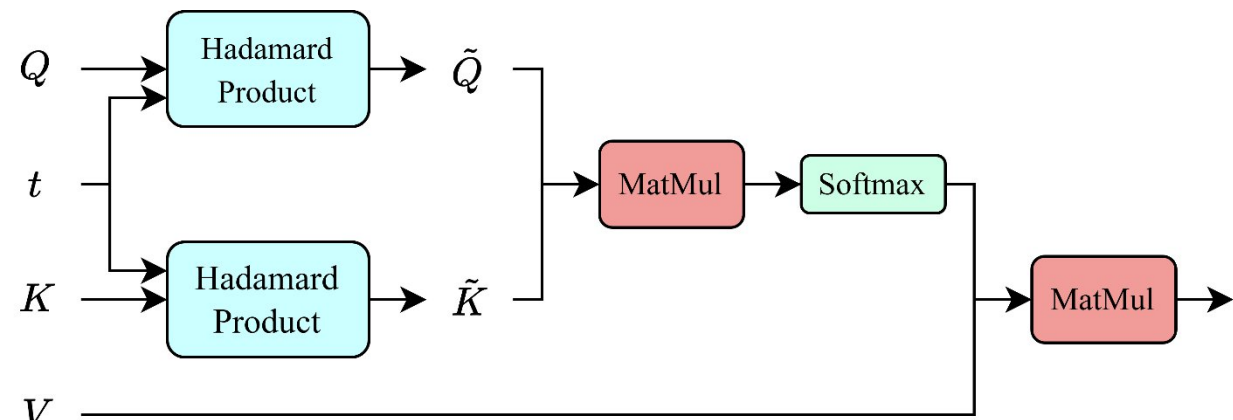
Proposed new TRINet cancer risk prediction model



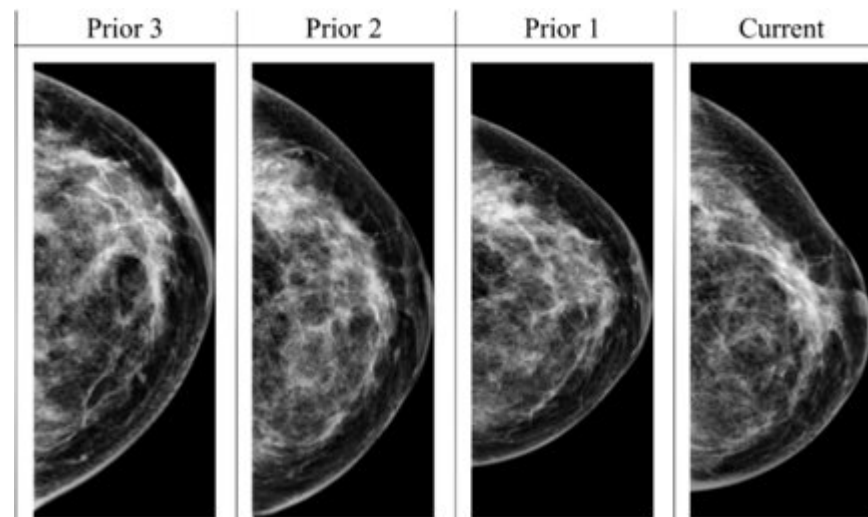
Proposed new Time-decay (TD) attention mechanisms

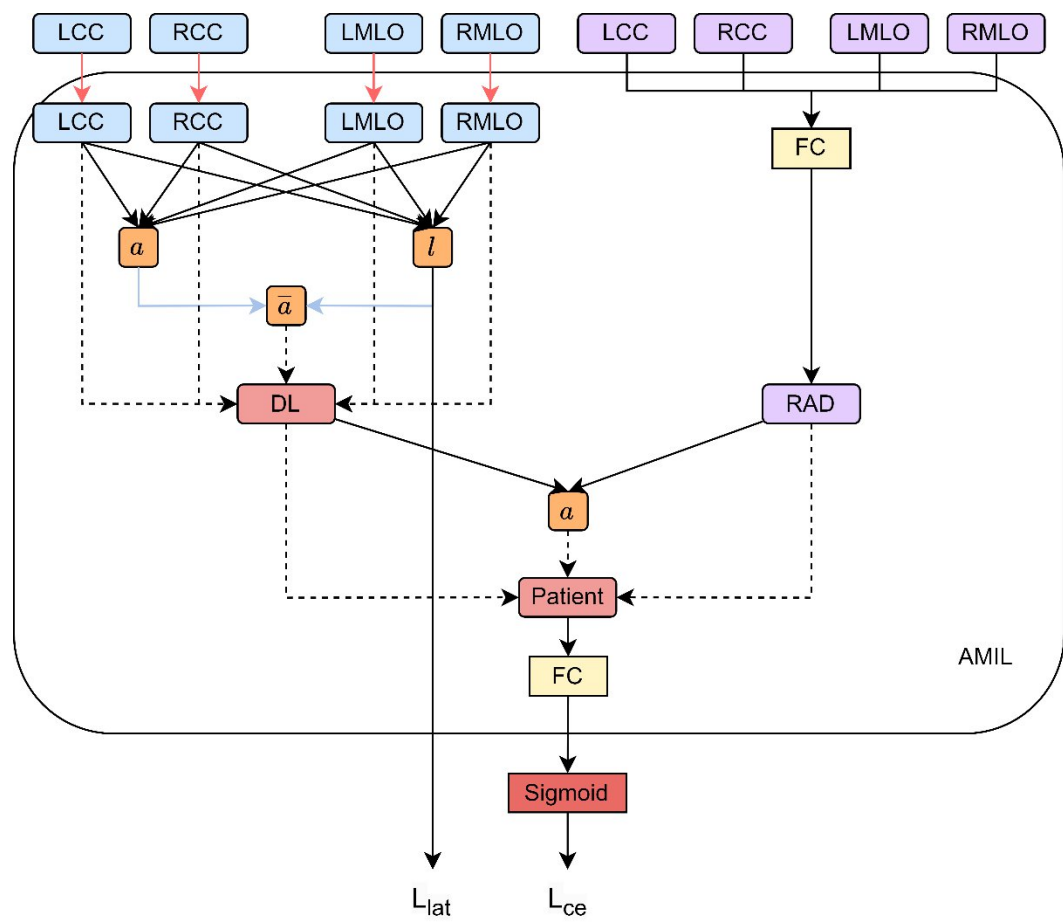


TD-SHIFT attention block



TD-NL attention block

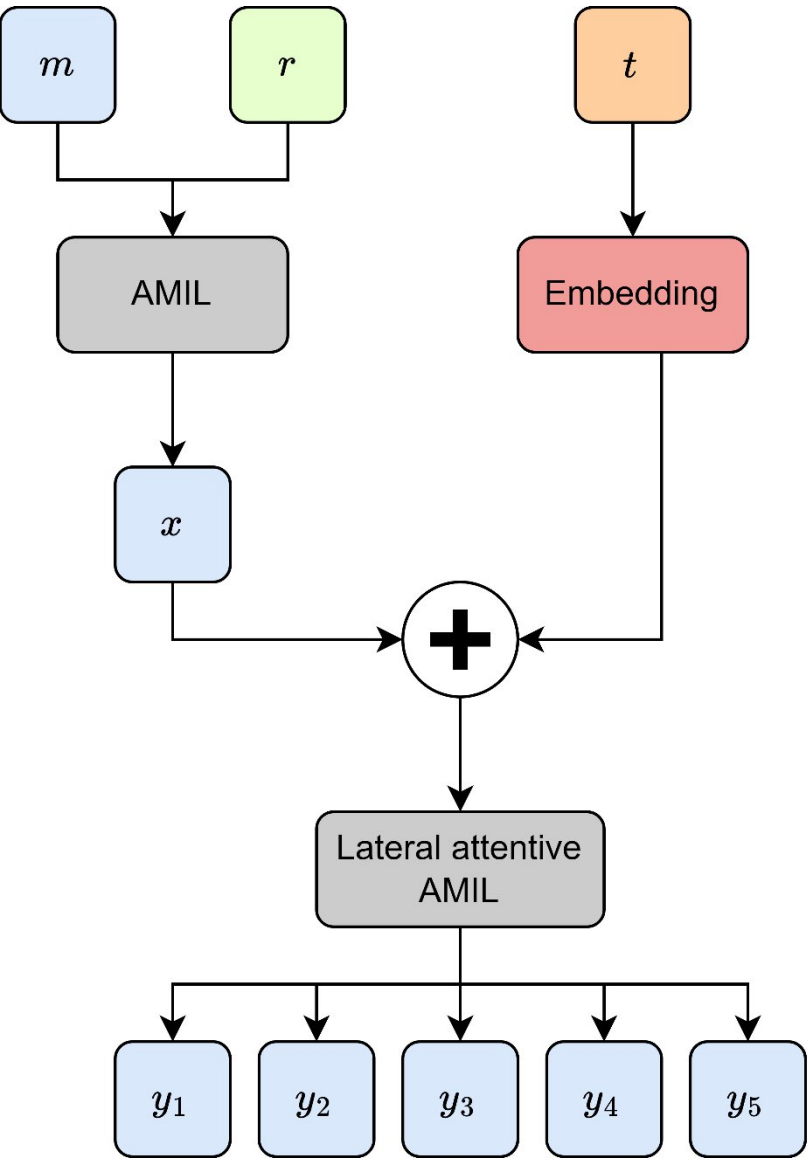




- DL features
- Rad features
- Attention weights
- Hybrid/Bag-level features
- FC Fully-connected layer
- AVG Mean
- Sigmoid
- L_{ce} Cross-entropy loss
- L_{lat} Lateral loss
- Downsample
- Weighted sum
- Attention weight combine

Radiomics and deep learning feature-based multiple instance learning (RADMIL) method combined with lateral attention

Proposed new Cancer forecast network with time-interval embeddings



Additive hazard layer with time-interval screening embeddings. The deep learning features, m are combined with radiomic features, r by our lateral-attentive AMIL based method. Then, the resulting feature embedding x is added with the screening time-interval t embedding, to form an additive hazard for future cancer risk prediction

Table 1
Detailed demographics for the EMBED dataset. We employed a five-fold cross-validation method, whereby the training and validation dataset was divided into five subsets, ensuring each subset was used for both training and validation at different iterations. The test set remained independent and was unseen during training.

Characteristics	EMBED training and validation sets		p-value	EMBED testing set		p-value
	Controls	Cases		Controls	Cases	
All examinations	6528	575	0.02	1308	117	0.02
Age						
<40	31	42		5	6	
40 - 50	1085	118		211	22	
50 - 60	1804	143		334	31	
60 - 70	1817	141	0.12	398	32	0.09
70 - 80	1423	101		282	21	
80+	368	30		78	5	
Tissue density						
Almost entirely fatty	702	40		140	7	
Scattered fibroglandular densities	2812	212	0.14	554	40	0.12
Heterogeneously dense	2653	286		552	62	
Extremely dense	347	34		61	8	
Unknown	14	3		1	0	
Race						
African American or Black	2927	271		583	56	
American Indian or Alaskan Native	14	1		2	0	
Asian	366	33		65	6	
Caucasian or White	2828	247		585	51	
Native Hawaiian	60	4		12	1	
Other Races	333	19		61	3	

Table 2
Demographic and LIBRA percent densities (Keller et al., 2012) for the CSAW dataset. We employed a five-fold cross-validation method, whereby the training and validation dataset was divided into five subsets, ensuring each subset was used for both training and validation at different iterations. The test set remained independent and was unseen during training. This dataset is heavily censored and only contains publicly released information on age and LIBRA percent density.

Characteristics	CSAW Training and validation sets		p-value	CSAW Testing set		p-value
	Controls	Cases		Controls	Cases	
All examinations	6279	695	<0.01	1571	178	<0.01
Age						
40 - 55	3084	255		769	64	
55+	3195	440	0.35628	802	114	0.26982
LIBRA percent density						
Mean	24.29	24.48		24.07	26.35	
Min	0.67	1.55		0.97	1.67	
Max	96.55	94.52		94.75	72.95	

Except for age, no significant differences between cancer and control cases in both datasets

Table 3: AUC results with 95 % CIs for the integration of radiomic features using different combination methods

Feature Combination Method	1-year AUC	2-year AUC	3-year AUC	4-year AUC	5-year AUC
FC	0.833 (0.789–0.877)	0.794 (0.745–0.846)	0.791 (0.745–0.839)	0.788 (0.748–0.831)	0.786 (0.744–0.831)
RADMIL	0.852 (0.808–0.901)	0.807 (0.756–0.859)	0.795 (0.751–0.842)	0.791 (0.747–0.837)	0.788 (0.746–0.833)
RADMIL + Lat	0.851 (0.806–0.904)	0.811 (0.764–0.862)	0.796 (0.751–0.839)	0.793 (0.751–0.84)	0.789 (0.743–0.831)

Table 4: AUC results with 95 % CIs of risk prediction using an additive hazard layer and additive hazard layer combined with time embeddings

Forecast Prediction Method	1-year AUC	2-year AUC	3-year AUC	4-year AUC	5-year AUC
Additive Hazard (Yala et al., 2021b)	0.857 (0.821–0.895)	0.814 (0.776–0.853)	0.796 (0.759–0.838)	0.783 (0.744–0.821)	0.780 (0.744–0.817)
Additive Hazard + Time Embedding	0.865 (0.836–0.915)	0.817 (0.785–0.87)	0.802 (0.763–0.846)	0.779 (0.74–0.82)	0.778 (0.737–0.819)

Table 5: Ablation study results compilation of incorporating new additions to our model.

Method	1-year AUC	2-year AUC	3-year AUC	4-year AUC	5-year AUC
Baseline	0.789 (0.746- 0.835) ($p < 0.01$)	0.756 (0.713- 0.799) ($p < 0.01$)	0.747 (0.704- 0.787) ($p = 0.01$)	0.737 (0.696- 0.780) ($p = 0.02$)	0.739 (0.697- 0.777) ($p = 0.02$)
SHIFT + T	0.825 (0.783–0.867) ($p < 0.01$)	0.784 (0.742–0.829) ($p < 0.01$)	0.771 (0.729- 0.816) ($p < 0.01$)	0.764 (0.725–0.805) ($p < 0.01$)	0.76 (0.721–0.8) ($p < 0.01$)
RADMIL (E)	0.852 (0.808–0.901) ($p < 0.01$)	0.807 (0.756–0.859) ($p < 0.01$)	0.795 (0.751–0.842) ($p < 0.01$)	0.791 (0.747–0.837) ($p < 0.01$)	0.788 (0.746–0.833) ($p = 0.01$)
RADMIL (E) + Lat	0.851 (0.806–0.904) ($p < 0.01$)	0.811 (0.764–0.862) ($p < 0.01$)	0.796 (0.751–0.839) ($p < 0.01$)	0.793 (0.751–0.84) ($p < 0.01$)	0.789 (0.743–0.831) ($p < 0.01$)
Additive Hazard + Time Embedding	0.865 (0.836–0.915) ($p < 0.01$)	0.817 (0.785–0.87) ($p < 0.01$)	0.802 (0.763–0.846) ($p < 0.01$)	0.779 (0.74–0.82) ($p = 0.02$)	0.778 (0.737–0.819) ($p = 0.04$)
ReST ^{CL} : (1st Iteration)	0.8549 (0.815–0.904) (referent)	0.8139 (0.769–0.863) (referent)	0.8014 (0.759–0.851) (referent)	0.7971 (0.754–0.841) (referent)	0.7934 (0.752-0.838) (referent)

Table 6: Comparison of AUC results with 95% CIs and C-indices with other SOTA methods

Method	C-index	1-year AUC	2-year AUC	3-year AUC	4-year AUC	5-year AUC
Mirai (Yala et al., 2021a) (Reported)	0.77 (0.75–0.79)	0.83 (0.81–0.86)	0.79 (0.77–0.82)	0.77 (0.75–0.80)	0.77 (0.75–0.79)	0.76 (0.74–0.79)
AsymMirai (Donnelly et al., 2024) (Reported)	Not reported	0.79 (0.73- 0.85)	0.69 (0.65–0.73)	0.68 (0.65- 0.71)	0.67 (0.64- 0.70)	0.66 (0.63- 0.69)
Lomar (Karaman et al., 2024)	0.708 (0.659 - 0.757)	0.836 (0.778–0.895)	0.768 (0.713–0.826)	0.746 (0.692–0.802)	0.725 (0.67–0.784)	0.715 (0.662–0.771)
Mirai (Yala et al., 2021b) (Reimplemented)	0.751 (0.715 - 0.788)	0.804 (0.761–0.852)	0.794 (0.756–0.837)	0.798 (0.759–0.838)	0.786 (0.749–0.827)	0.787 (0.746–0.824)
TRINet	0.780 (0.741 - 0.818)	0.8549 (0.815–0.904)	0.8139 (0.769–0.863)	0.8014 (0.759–0.851)	0.7971 (0.754–0.841)	0.7934 (0.752–0.838)

Published Journal Paper:

No:	Paper title:	Author names	Affiliations	Journal name:	The publisher of the Journal	The volume number and Pages
1	A new time-decay radiomics integrated network (TRINet) for breast cancer risk prediction	Hong Hui Yeoh, Fredrik Strand, Raphaël Phan, Kartini Rahmat, Maxine Tan	Monash University Malaysia, Karolinska Institute, University of Malaya	Medical Image Analysis, ISI: Q1, IF: 11.8	Elsevier	2026, Vol. 107, Pages 103829

Submitted Journal Paper:

No:	Paper title:	Author names	Affiliations	Journal name:	The publisher of the Journal	The volume number and Pages
1	A multi-radiomics deep learning based breast cancer risk prediction model using sequential mammographic images with image attention and bilateral asymmetry refinement	Hong Hui Yeoh, Andrea Liew, Raphaël Phan, Fredrik Strand, Kartini Rahmat, Tuong Linh Nguyen, John L. Hopper, Maxine Tan	Monash University Malaysia, Karolinska Institute, University of Malaya, The University of Melbourne	Physics in Medicine and Biology, ISI: Q1, IF: 3.4	Elsevier	Under review, Moderate revision

Societal impact of project:

- Breakthrough towards early cancer detection
- Risk assessment model for individualized risk
- Personalized screening recommendations for women
- Reduced patient mortality rates
- Reduced false-positives, over-diagnosis, and high healthcare costs through unnecessary biopsies, etc.

Conclusions:

- Using time-decay attention-based screenings improves risk prediction performance
- New RADMIL method effectively combines radiomic and deep learning features over different views
- New time embedding layer allows the model to account for the timing of previous screenings, improving future cancer risk prediction
- Using 2 comprehensive public databases (8,528 patients from American EMBED dataset and 8,723 patients from Swedish CSAW dataset), new risk model outperforms state-of-the-art methods in literature

Future work:

- Only able to test on two public datasets of American (EMBED) and Swedish (CSAW) populations, which may limit generalizability
- Need for broader clinical testing and validation on more diverse patient datasets in the future
- If possible, perform clinical testing on model's utility and impact in assisting radiologists